



# Exosomal miR-30a-5p targets NLRP3 to suppress podocyte pyroptosis in diabetic nephropathy

WEI LU<sup>1,\*</sup>; KAN GUO<sup>2</sup>; DIANMEI XI<sup>1</sup>; ZHAOXIA XIA<sup>1</sup>

<sup>1</sup> Department of Endocrinology and Metabolism, Luzhou People's Hospital, Luzhou, 646000, China

<sup>2</sup> Key Laboratory of Epigenetics and Oncology, The Research Center for Preclinical Medicine, Southwest Medical University, Luzhou, 646000, China

**Key words:** Diabetic nephropathy, Podocyte, Pyroptosis, Exosomal miR-30a-5p, NLRP3

**Abstract: Background:** Mesenchymal stem cell (MSC)-derived exosomes are closely related to pyroptosis in diabetic nephropathy (DN). This study aimed to explore the protective effect of exosomal miR-30a-5p on podocyte pyroptosis in DN. **Methods:** Streptozotocin was used to establish the mouse model of DN. Human bone marrow MSC-derived exosomes were extracted and identified via transmission electron microscopy, nanoparticle tracking analysis, and western blotting. MiR-30a-5p mimics and non-control (NC) mimics were transfected into MSCs and podocytes, and exosomes were isolated from the MSCs. High glucose (HG)-induced podocyte model was established to determine the effect of exosomal miR-30a-5p on pyroptosis and inflammation *in vitro*. **Results:** MiR-30a-5p was expressed at low levels in DN models, while NLR family pyrin domain containing 3 (NLRP3), caspase-1, gasdermin-N (GSDMD-N), and pro-inflammatory factors (tumor necrosis factor- $\alpha$ , interleukin (IL)-1 $\beta$ , and IL-18) were augmented. *In vitro*, miR-30a-5p expression in the HG-damaged podocytes was down-regulated, while NLRP3 was up-regulated. Interestingly, miR-30a-5p overexpression diminished HG-induced podocyte injury, as proven by increased activity and decreased pyroptosis of podocytes. Concurrently, the up-regulation of miR-30a-5p could inhibit the expression of pro-inflammatory factors, caspase-1, GSDMD-N, and NLRP3 in HG-induced podocytes. MSC-derived exosomal miR-30a-5p treatment of HG-damaged cells has similar effects to miR-30a-5p mimics treatment. Overexpression of NLRP3 reversed the effect of miR-30a-5p mimics on HG-induced podocytes. **Conclusion:** This research confirmed that exosomal miR-30a-5p regulates pyroptosis via mediating NLRP3 in DN.

## Introduction

Diabetic nephropathy (DN) accounts for 1/3 to 1/2 of the cases of end-stage renal disease and has become a threat to people's health worldwide (Umanath & Lewis, 2018). The early pathological manifestations of DN include thickening of the glomerular basement membrane (GBM), slight dilatation of mesangium, and arteriolar accumulation of hyaline (Najafian *et al.*, 2011). The sign of DN development is the gradual onset of proteinuria caused by the decrease in glomerular filtration rate; podocyte injury is an important cause of decreased glomerular filtration rate (Podgórski *et al.*, 2019). Podocytes are highly differentiated cells attached to GBM and are important in maintaining renal function (Pavenstädt *et al.*, 2003). Because of its limited proliferative ability, the separation and apoptosis of

podocytes from GBM inevitably reduce podocyte density, impairing glomerular filtration function and increasing proteinuria (Wharram *et al.*, 2005). Studies have shown that podocyte injury and loss contribute to the progression of DN (Assady *et al.*, 2017; Hong *et al.*, 2018; Lal & Patrakka, 2018). Podocyte dysfunction caused by high glucose (HG) plays a major role in DN (Ito *et al.*, 2017). Therefore, it is critical to study the possible targets of DN based on podocytes to develop new ways of treating and preventing DN.

MicroRNAs (miRNAs) are involved in many pathophysiological processes and diseases (Bartel, 2004; Yang *et al.*, 2022). They can bind to the 3'-untranslated region of one or more downstream genes and regulate the levels of target genes (Eulalio *et al.*, 2008; Filipowicz *et al.*, 2008). For example, miR-199a-3p directly acts on the inhibitor of nuclear factor kappa-B kinase subunit beta (IKK- $\beta$ ) to attenuate apoptosis and inflammation of renal tubular epithelial cells in DN (Zhang *et al.*, 2020).

\*Address correspondence to: Wei Lu, lzsrmyyluwei@163.com

Received: 07 February 2023; Accepted: 26 May 2023



According to [Ding et al. \(2020\)](#), miR-21-5p targets A20 to regulate the damage of DN podocytes. MiR-30 is abundantly expressed in podocytes, and its down-regulation promotes glomerulosclerosis and podocyte apoptosis ([Wu et al., 2014](#); [Liu et al., 2016](#); [Zhao et al., 2017a](#); [Lang et al., 2019](#)). Overexpression of miR-30 can reduce the apoptosis of podocytes induced by HG ([Liu et al., 2016](#)). Therefore, we speculate that miR-30a-5p is directly associated with podocyte damage in DN.

Exosomes produced by mesenchymal stem cells (MSCs) have the potential to be a novel therapeutic approach for the management of DN ([Xiong et al., 2021](#)). The miRNAs loaded in exosomes are closely related to the development of DN ([He et al., 2021](#)). Exosomes from adipose-derived MSCs, containing miR-125a, inhibit the progress and alleviate symptoms of DN ([Hao et al., 2021](#)). MiR-424-5p derived from MSC-exosomes attenuates diabetic kidney disease by inhibiting cell apoptosis and epithelial-to-mesenchymal transition ([Cui et al., 2022](#)). Thus, we postulated that exosomal miR-30a-5p secreted by MSCs might ameliorate DN.

NLR family pyrin domain containing 3 (NLRP3) is one of the inflammatory corpuscles located in cells, which can regulate the excitation of caspase-1 and indirectly regulate the maturation and secretion of interleukin (IL)-1 $\beta$  and IL-18, causing an inflammatory reaction and cell death ([Qiu & Tang, 2016](#); [Xin et al., 2018](#)). Recent evidence indicate the involvement of pyroptosis in the development of DN ([Liu et al., 2021](#); [Mamun et al., 2021](#); [Zuo et al., 2021](#)). Unlike apoptosis, pyroptosis involves programmed cell death caused by inflammatory caspase (mainly caspase-1), which is closely linked to the excitation of NLRP3 ([Man et al., 2017](#)). Activated caspase-1 cleaves gasdermin D (GSDMD) to produce the pore-forming N-terminus of GSDMD (GSDMD-N) to induce pyroptosis ([Wang et al., 2022](#)). The expression levels of pyroptosis-related proteins, including caspase-1, GSDMD-N, and NLRP3, are increased in diabetic kidney tissue ([Shahzad et al., 2015](#); [Gao et al., 2022](#)). The NLRP3 inflammatory complex senses and recognizes endogenous risk signals such as fatty acids and reactive oxygen species (ROS), initiating caspase-1 and IL-1 $\beta$ , thereby promoting DN progression induced by the inflammatory cascade ([An et al., 2020](#); [Yu et al., 2020](#)). These findings strongly suggest the role of NLRP3-mediated pyroptosis in DN progression. However, the specific molecular mechanism of NLRP3 in DN podocyte pyroptosis is not yet completely understood.

Although many studies indicate a significant role of the miR-30 family in DN ([Zhao et al., 2017b](#); [Dieter et al., 2019](#)), there have been limited studies showing the regulatory role of miR-30a-5p in DN targeting NLRP3. MiR-30b ameliorates DN by targeting Runt-related transcription factor-1 ([Zhang et al., 2021](#)), and miR-30c protects against DN by inhibiting epithelial-to-mesenchymal transition in db/db mice ([Zhao et al., 2017b](#)). Hence, this study explored the exosomal miR-30a-5p effect in the pathogenesis and mechanism of DN using the DN-mice and DN-podocytes as disease models. This work is expected to provide new evidence for understanding the occurrence and progression of DN and shed light on novel prevention and treatment measures for DN.

## Materials and Methods

### *Mice*

Twenty male Kunming mice (KM) (6–8 weeks) were purchased from Hunan SJA Laboratory Animal Co., Ltd. (China). DN model was established in mice by streptozotocin (STZ, Sigma, Darmstadt, Germany) induction. The mice were subject to a fasting period of 4~6 h and then injected with 50 mg/kg of STZ intraperitoneally daily for five days. The control group was treated with the same volume of citrate buffer. The DN model was determined to be successfully established when blood glucose levels increased to  $\geq 16.7$  mmol/L. Subsequently, all mice were euthanized under halothane anesthesia at the end of the experiments. All animal experiments complied with ARRIVE guidelines. This study was approved by the Hunan SJA Laboratory Animal Co., Ltd. (China) (ethics approval number IACUC-SJA2021019-4).

### *Extraction and identification of exosomes*

Human bone marrow MSCs were purchased from Pricella (Wuhan, China). MSCs were maintained in Dulbecco's modified Eagle medium (DMEM)/F-12 medium (Sigma, Darmstadt, Germany) containing 1% penicillin-streptomycin (Beyotime, Shanghai, China). Then, MSCs were grown in a serum-free medium for 2 days. Cell supernatants of MSCs were collected, and cell debris was removed by centrifugation at 3000 g for 15 min. The supernatants were mixed with exosome extraction reagent (System Biosciences, Palo Alto, USA) in a ratio of cell supernatant:ExoQuick TC = 5:1, and the mixture was fully mixed and left overnight at 4°C. The mixture was centrifuged with 1500 g for 30 min to separate the exosomes from the cell culture. For exosome characterization, nanoparticle tracking analysis (NTA) and transmission electron microscopy (TEM) analysis were performed following the protocol in a previous study ([Jiang et al., 2021](#)). Exosomal markers, including CD63, HSP70, and calnexin, were determined by western blotting.

### *Uptake of exosomes*

The extracted exosomes were stained with Dil dye solution (AmyJet Scientific Inc., Wuhan, China). Stained exosomes (20  $\mu$ g) were added to the cell culture medium and incubated with MPC5, and the fluorescence status was checked under a fluorescence microscope (AE31E, Motic, Baltimore, USA) and photographed and recorded.

### *Cells culture*

Mouse Podocyte Clone-5 (MPC5, Tongpai, Shanghai, China) was cultured in a DMEM medium (D5796, Sigma, Darmstadt, Germany) (containing 10% fetal bovine serum + 1% double resistance). MPC5 was treated with 0, 10, 20, and 30 mM glucose for 48 h. MPC5 was cultured with 30 mmol/L glucose for 0, 12, 24, 36, and 48 h. MPC5 treated with 30 mM glucose medium for 48 h was considered the high glucose group (HG). MPC5 cultured in DMEM containing 5.5 mM glucose was considered the control group (NC). Mannitol-treated MPC5 acted as an osmotic pressure control group (MA).

### Cell transfection

Lipofectamine 3000 (Invitrogen, Carlsbad, USA) was used for transient transfection. MiR-30a-5p mimics, a NLRP3 overexpression plasmid, and their corresponding negative controls were used for transfection in the HG-induced MPC5 group. The experiments are grouped as follows: NC group, HG group, HG + mimics NC group, HG + miR-30a-5p mimics group, and the HG group, HG + mimics NC + oe-NC group, HG + miR-30a-5p mimics group, HG + oe-NLRP3 group, HG + miR-30a-5p mimics + oe-NLRP3 group.

### MSC-exos treatment of mouse podocyte clone-5

The cells were grouped into: Control group (MPC5 was cultivated with normal glucose), HG group (HG-induced MPC5), MSC-EXOs group (the exosomes that were isolated from MSCs were used to treat HG-induced MPC5), MSC-EXOs mimics NC group (the exosomes separated from MSCs were transfected with NC mimics and used to treat HG-induced MPC5), MSC-EXOs miR-30a-5p mimics group (the exosomes separated from MSCs were transfected with miR-30a-5p mimics and used to treat HG-induced MPC5).

### Quantitative reverse transcription polymerase chain reaction (RT-qPCR)

Total RNA was extracted from renal tissues, MPC5, and exosomes using Trizol reagent (Invitrogen, Carlsbad, USA). RNA quality was assessed using a NanoDrop2000 spectrophotometer (Thermo Fisher Science, Waltham, USA). The RNA was transcribed into cDNA using an mRNA reverse transcription Kit (CW2569, CWBIO, Beijing, China). Primers designed for RT-qPCR are mentioned in Table 1. RT-qPCR was carried out at 95°C for 10 min, 95°C for 15 s, and 60°C for 30 s. The  $2^{-\Delta\Delta Ct}$  method was used for analysis, and  $\beta$ -actin and U6 were used as internal references to calculate the relative expression of the target gene.

### Western blotting

Protein from renal tissues and MPC5 was extracted using RIPA lysis buffer (Beyotime Shanghai, China) containing phosphatase inhibitor (P1260, Applygen, Beijing, China) and protease inhibitor (583794, Gentihold, Beijing, China). The protein sample was mixed with the loading buffer and heated at 95°C to 100°C for 5 min. The protein was

separated by sodium dodecyl sulfate-polyacrylamide gel electrophoresis and transferred onto a nitrocellulose membrane. For blocking the membrane, 5% skim milk was used for 1 h at room temperature. Primary antibodies, anti-NLRP3 (1:1000, ab214185, Abcam, Cambridge, UK), anti-GSDMD-N (1:1000, ab215203, Abcam, Cambridge, UK), anti-caspase-1 (1:1000, 22915-1-AP, Proteintech, Rosemont, USA), anti-IL-1beta (1:2000, #12703, CST, Danvers, USA), anti-IL-18 (1:1000, 10663-1-Ap, Proteintech, Rosemont, USA), and anti- $\beta$ -actin (1:5000, 66009-1-Ig, Proteintech, Rosemont, USA) were added to the membranes and kept overnight at 4°C. Secondary antibodies were added to react with the membranes for 2 h. The membranes were incubated with SuperECL Plus (Advansta, San Jose, USA) for 5 min and then visualized on a chemiluminescence imaging system (Chemiscope 6100, Qinxiang, Guangzhou, China).

### Immunofluorescence

Renal tissues were paraffin-embedded and sectioned. The sections were heated at 60°C for 12 h. The sections were dehydrated in xylene and ethanol and then microwave heated by immersing them in ethylenediamine tetraacetate buffer for 24 min. The sections were placed in sodium borohydride solution for 30 min. The sections were soaked in 75% ethanol solution for 15 s~1 min and placed in Sudan black staining solution for 15 min. The sections were incubated with 5% bovine serum albumin (BSA) for 60 min, followed by primary antibody (1:50, Nephrin, ab216341; GSDMD-N, ab219800, Abcam, Cambridge, UK) at 4°C overnight. The sections were then incubated with secondary antibodies at 37°C for 60~90 min. The nuclei were stained with 4',6-diamidino-2-phenylindole (DAPI) at 37°C for 10~20 min. The sections were sealed with buffered glycerol and observed under a fluorescence microscope.

MPC5 on glass slides was fixed with 4% paraformaldehyde for 30 min. Triton (0.3%) was added to the glass slides and permeabilized for 30 min. BSA (5%) was added to the glass slides and incubated for 30 min. The slides were then incubated with primary antibody GSDMD-N (1:50, ab215203, Abcam, Cambridge, UK) and caspase-1 (1:50, 22915-1-AP, Proteintech, Rosemont, USA) at 4°C, overnight. Then, the cell slides were treated with secondary antibodies in a dark room for 1 h. Slides were treated with DAPI for 10 min. Next, the cells were sealed with buffered glycerol and observed under a fluorescence microscope.

### Enzyme-linked immunosorbent assay (ELISA)

ELISA kits were purchased from Cusabio Biotech Co., Ltd. (Wuhan, China) to measure the protein levels of tumor necrosis factor (TNF)-alpha (CSB-E04741m), IL-1beta (CSB-E08054m), and IL-18 (CSB-E04609m) in serum and cell supernatant. Samples and standards were processed according to the manufacturer's instructions.

### Cell Counting Kit-8 (CCK-8)

The cell viability of MPC5 was evaluated by CCK-8 assay (NU679, Dojindo Molecular Technologies, Inc., Kumamoto, Japan) according to the manufacturer's protocol. The cells

TABLE 1

#### Primer sequences

Gene	Sequences (5'-3')
NLRP3	F: CCTCTTTGGCCTTGTAACACAG R: TGGCTTTCACTTCAATCCACT
miR-30a-5p	F: GCGACTGTAAACATCCTCGAC R: CAGCTGCAAACATCCGACTG T
$\beta$ -actin	F: ACATCCGTAAAGACCTCTATGCC R: TACTCCTGCTTGCTGATCCAC
U6	F: CTCGCTTCGGCAGCACA R: AACGCTTCACGAATTTGCGT

were seeded in 96-well plates at  $5 \times 10^3$  cells/well density. CCK8 solution (10  $\mu$ L) was added to each well. After incubation at 37°C, 5% CO<sub>2</sub> for 4 h, the absorbance was measured at 450 nm using a Bio-Tek microplate.

#### Flow cytometry detection

A caspase-1 (active) staining assay kit (ab219935, Abcam, Cambridge, UK) was used to detect the pyroptosis of MPC5.  $5 \times 10^5$  MPC5 were digested by trypsin and then incubated with FAM-YVAD-FMK solution for 1 h. The cells were treated with propidium iodide staining buffer for 10 min. The flow cytometer (A00-1-1102, Beckman, Brea, USA) was used to detect the fluorescence intensity.

#### Luciferase assay

The TargetScan software was used to predict that NLRP3 interacts with miR-30a-5p, and this was verified using the dual-luciferase reporter system. Briefly, NLRP3-wt and miRNA-NC or miR-30a-5p mimics, NLRP3-mut and miRNA-NC or miR-30a-5p-mimics were transfected into 293A cells using the Lipofectamine 3000 Kit (Invitrogen, Carlsbad, USA). The luciferase activity was detected by a dual-luciferase reporter assay kit (E1910, Promega, Madison, USA).

#### Statistical analysis

All experiments were carried out three times independently. The data were statistically analyzed by GraphPad Prism 8 software (GraphPad software, La Jolla, USA). The statistical significance between the two groups was determined by an unpaired *t*-test. The statistical significance of the difference between three or more groups was determined by One-way ANOVA. *p* < 0.05 was regarded as statistically significant, and all data were expressed as mean  $\pm$  SD.

## Results

#### Detection of miR-30a-5p, pyroptosis-related proteins, and inflammatory factors in diabetic nephropathy mice

DN mice models were established by STZ injection. Compared with the control mice, the miR-30a-5p level was down-regulated in DN mice, and the NLRP3 level was up-regulated (Figs. 1A–1B). Western blotting also verified that the protein levels of caspase-1, GSDMD-N, IL-1beta, and IL-18 were considerably augmented in DN mice than in control mice (Fig. 1B). The immunofluorescence results showed enhanced expression of GSDMD-N in the DN model (Fig. 1C). Nephritin expression was decreased, while TNF-alpha, IL-18, and IL-1beta levels in the serum of DN mice increased compared to those in control mice (Fig. 1D). These results indicated that the down-regulation of miR-30a-5p expression might be related to increased pyroptosis and inflammation in DN.

#### Detection of miR-30a-5p and NLR family pyrin domain containing 3 in high-glucose-induced podocytes

We used high glucose conditions to treat MPC5 and simulate DN and then measured miR-30a-5p and NLRP3 mRNA levels in MPC5 exposed to different glucose concentrations (0, 10,

20, and 30 mM). The level of miR-30a-5p in podocytes decreased in a dose-dependent manner (Fig. 2A). In contrast, the level of NLRP3 increased. In MPC5 exposed to 30 mM glucose (0, 12, 24, 36, and 48 h), miR-30a-5p expression decreased, while that of NLRP3 increased in a time-dependent manner (Fig. 2B). The comparison revealed that MPC5 treated with NC or mannitol (MA), miR-30a-5p expression in MPC5 treated with HG was down-regulated, and NLRP3 was up-regulated (Fig. 2C). The above results further verified that miR-30a-5p and inflammatory corpuscle NLRP3 have potential roles in DN.

#### Up-regulation of miR-30a-5p inhibited high-glucose-induced podocyte injury

To study the effect of miR-30a-5p in HG-induced MPC5 injury, we transfected HG-induced MPC5 with miR-30a-5p mimics. RT-qPCR result confirmed the efficiency of miR-30a-5p up-regulation (Fig. 3A). CCK 8 results verified that cell viability decreased when exposed to HG but this was reversed by the transfection of miR-30a-5p mimics (Fig. 3B). Flow cytometry demonstrated that up-regulation of miR-30a-5p reduced HG-induced podocyte pyroptosis (Fig. 3C). Immunofluorescence analysis showed that miR-30a-5p mimics reversed HG-induced up-regulation of caspase-1 and GSDMD-N (Fig. 3D). TNF-alpha, IL-18, and IL-1beta levels were higher in the supernatant of MPC5 treated with HG compared with the NC group, and miR-30a-5p overexpression could significantly reduce the secretion of these inflammatory factors (Fig. 3E). The above results show that miR-30a-5p could modulate the pyroptosis and inflammation of MPC5 in DN.

#### NLR family pyrin domain containing 3 directly targets miR-30a-5p

Next, we verified the target relationship between miR-30a-5p and the inflammasome NLRP3. Bioinformatic analysis predicted the binding sites of miR-30a-5p and NLRP3 (Fig. 4A). In the luciferase assay, the luciferase activity of MPC5 transfected with miR-30a-5p mimics in the NLRP3-wt group was considerably lower than that of MPC5 cells transfected with mimics-NC. Meanwhile, the luciferase activity of MPC5 transfected with miR-30a-5p mimics or NC mimics in the NLRP3-mut group did not differ significantly (Fig. 4B). The expression of NLRP3 in HG-induced podocytes was decreased by the transfection of miR-30a-5p mimics (Figs. 4C–4D). The data indicate that NLRP3 may target and inhibit the expression of miR-30a-5p in MPC5.

#### Overexpression of NLR family pyrin domain containing 3 reverses the effects of miR-30a-5p on podocyte injury

Next, we studied the effects of overexpression of NLRP3 and miR-30a-5p on podocyte damage. NLRP3 was overexpressed in MPC5, and RT-qPCR was used to verify the overexpression efficiency (Fig. 5A). After transfection of HG-induced MPC5 with miR-30a-5p mimics, the cell viability increased, and the pyroptosis rate decreased as compared to those in the NC-mimics group (Figs. 5B–5C). After the transfection of oe-NLRP3, the above results were reversed (Figs. 5B–5C). Compared to the NC-mimics group,

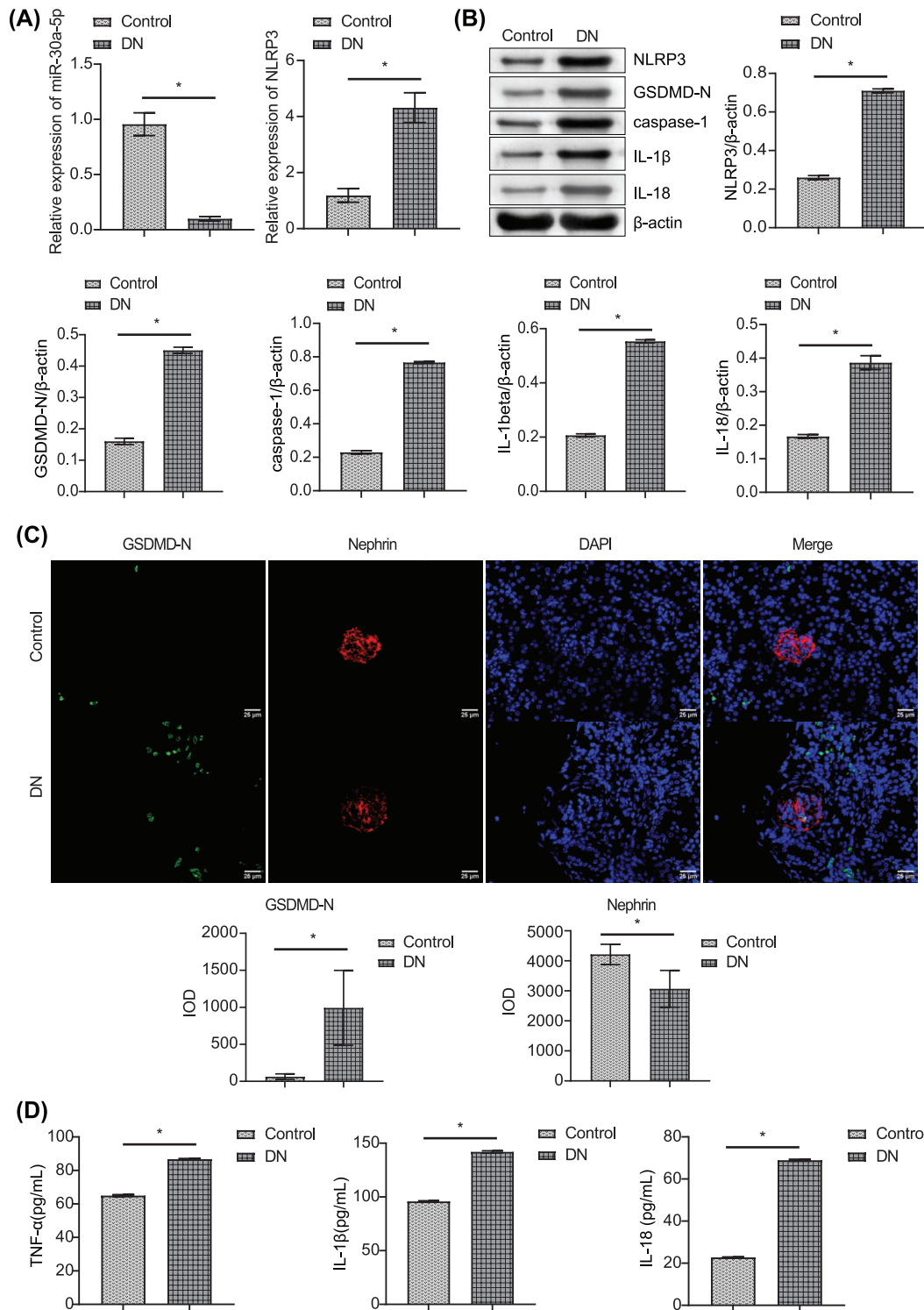


**FIGURE 1.** Detection of miR-30a-5p, pyroptosis-related proteins, and inflammatory factors in DN mice. (A) miR-30a-5p and NLRP3 mRNAs in the kidney were assayed by RT-qPCR in the kidney. (B) NLRP3, GSDMD-N, caspase-1, IL-1beta, and IL-18 levels were assayed by RT-qPCR in the kidney. (C) Immunofluorescence was used to determine the level of GSDMD-N and Nephryn in the kidney. Scale bar = 25 μm. (D) ELISA was performed to detect the changes in TNF-alpha, IL-18, and IL-1beta in serum. \* $p < 0.05$ . Each assay was repeated thrice, with three biological replicates. DN, diabetic nephropathy; RT-qPCR, Quantitative reverse transcription polymerase chain reaction; ELISA, enzyme-linked immunosorbent assay; NLRP3, NLR family pyrin domain containing 3; GSDMD-N, gasdermin-N; IL-1β, interleukin-1beta; TNF, tumor necrosis factor.

NLRP3, and caspase-1 were significantly descended in MPC5 transfected with miR-30a-5p mimics. Oe-NLRP3 transfection increased the expression levels of these proteins (Fig. 5D). Immunofluorescence results verified that the changing trend

of caspase-1 was similar to the above results (Fig. 5E). The levels of TNF-alpha, IL-18, and IL-1beta in the cell supernatant of the oe-NLRP3 group and the miR-30a-5p mimics+oe-NLRP3 group were significantly higher than in

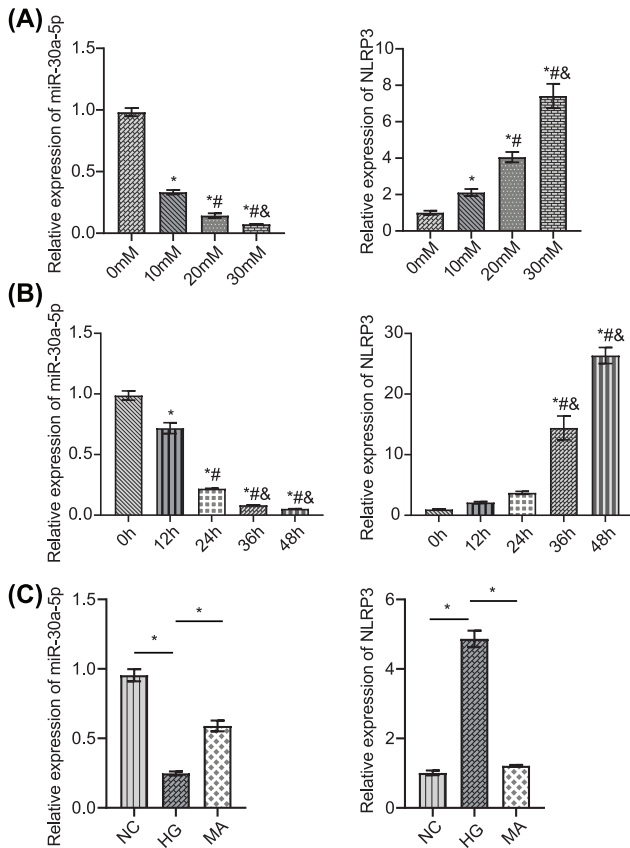


**FIGURE 2.** Detection of miR-30a-5p and NLRP3 in podocytes. (A) MPC5 was induced by different concentrations of glucose (0, 10, 20, and 30 mM for 48 h). MiR-30a-5p and NLRP3 levels were measured in MPC5. \* vs. 0 mM. # vs. 10 mM. & vs. 20 mM.  $p < 0.05$ . (B) MPC5 was treated with 30 mM glucose for 0, 12, 24, 36, and 48 h, respectively. miR-30a-5p and NLRP3 were measured in MPC5. \* vs. 0 h; # vs. 12 h; & vs. 24 h.  $p < 0.05$ . (C) miR-30a-5p and NLRP3 levels were quantified by RT-qPCR. \* $p < 0.05$ . Each assay was repeated thrice, with three biological replicates. MPC5, Mouse Podocyte Clone-5; RT-qPCR, Quantitative reverse transcription polymerase chain reaction; NLRP3, NLR family pyrin domain containing 3.

the miR-30a-5p mimics group (Fig. 5F). The above results suggested that NLRP3 overexpression could reverse the effects of the miR-30a-5p on HG-induced MPC5.

#### Mesenchymal stem cell-derived exosomal miR-30a-5p can be taken up by podocytes

We extracted exosomes from MSCs. TEM and NTA assays revealed that the exosomes were cup-shaped, and their diameters ranged from 100 to 200 nm (Figs. 6A and 6B). The expression of CD63, HSP70, and calnexin in exosomes was examined by western blot analysis. CD63 and HSP70 were enriched in exosomes, while calnexin was expressed at lower levels (Fig. 6C). MiR-30a-5p was highly expressed in exosomes (Fig. 6D). The exosome uptake assay showed that the loaded exosome miR-30a-5p could be taken up by the podocytes (Fig. 6E).

#### Mesenchymal stem cell-derived exosomes carrying miR-30a-5p inhibit podocyte pyroptosis by regulating NLR family pyrin domain containing 3

To investigate the effect of exosomes on podocytes, we treated podocytes with exosomes obtained from MSCs and transfected with miR-30a-5p mimics. RT-qPCR results showed a good overexpression efficiency of miR-30a-5p (Fig. 7A). The flow cytometry results showed that exosome intervention inhibited HG-induced pyroptosis of podocytes (Fig. 7B). Further detection of pyroptosis-related proteins showed that exosome treatment inhibited NLRP3, GSDMD-N, and caspase-1 expression in HG-induced cells (Fig. 7C). In addition, the secretion of inflammatory factors in HG-induced podocytes was reduced by exosome intervention (Fig. 7D). Overall, the exosomes released by miR-30a-5p mimics-treated MSCs had a stronger reversal effect as compared to MSC exosomes alone.

#### Discussion

At present, the treatment of DN is still a huge challenge, and the pathogenesis of DN has received more attention (Raval et al., 2020). Our study examined the potential effects of pyroptosis in DN models *in vivo* and *in vitro*. In this study, we discovered that pyroptosis, as well as inflammation modulated by miR-30a-5p/NLRP3 signal pathway, are involved in the progress of DN.

Here, miR-30a-5p was diminished in the kidney of DN model mice. Evidence shows that miRNAs play a critical role in DN (Yarahmadi et al., 2021). We established the podocyte injury model induced by HG and found that miR-30a-5p was diminished in a time and concentration-dependent manner. These results indicated that miR-30a-5p might be an essential target in DN. MiR-30a-5p has been recently shown to regulate inflammation through an indirect or direct mechanism and is negatively correlated with the level of pro-inflammatory cytokines; thus, negatively regulating inflammation (Caserta et al., 2017). Similarly, the expression levels of the miR-30 family in macrophages of high-fat diet-fed mice is down-regulated, which subsequently mediates Nox1 signal transduction to cause low-grade inflammation (Miranda et al., 2018). The latest evidence showed that miR-30a-5p attenuates the inflammatory reaction of rat podocytes by inhibiting *Becn1* expression and playing a protective role in DN (Yang et al., 2021). Our study reported that overexpression of miR-30a-5p could inhibit the pyroptosis and inflammation levels of HG-induced MPC5.

An outcome of inflammation-mediated caspase-1 activation, pyroptosis is considered another essential contributor to DN, consistent with DN's aseptic inflammation characteristics (Tesch, 2017). Studies have proved that caspase-1 deficiency inhibits the activation of inflammatory corpuscles and has a protective effect on DN (Shahzad et al., 2016). Our study demonstrated increased expression of pyroptosis-related proteins and pro-inflammatory cytokines

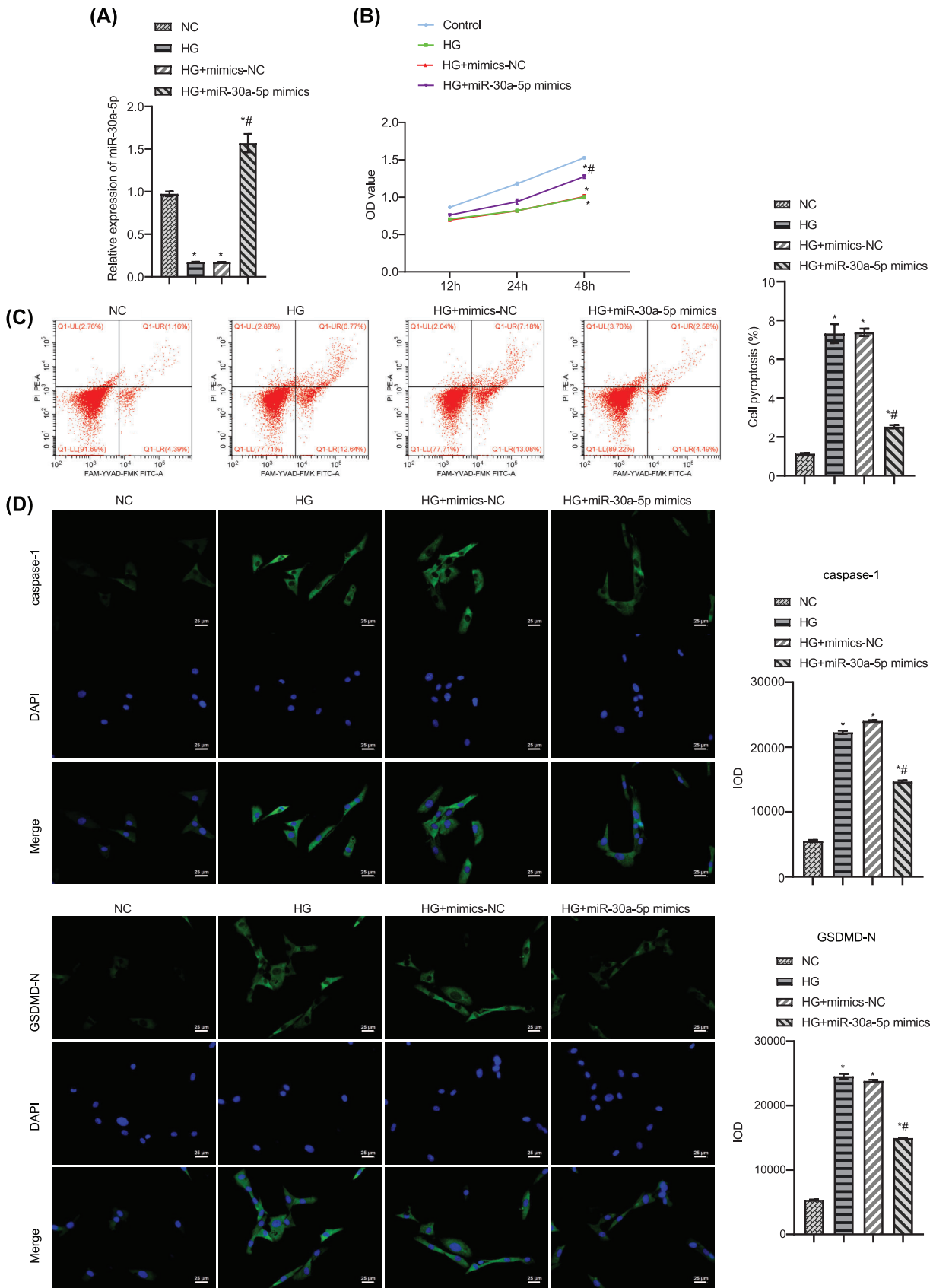
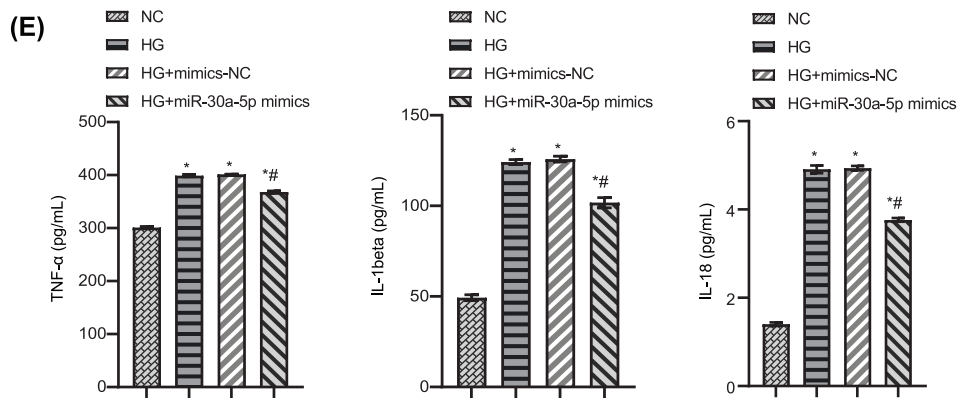
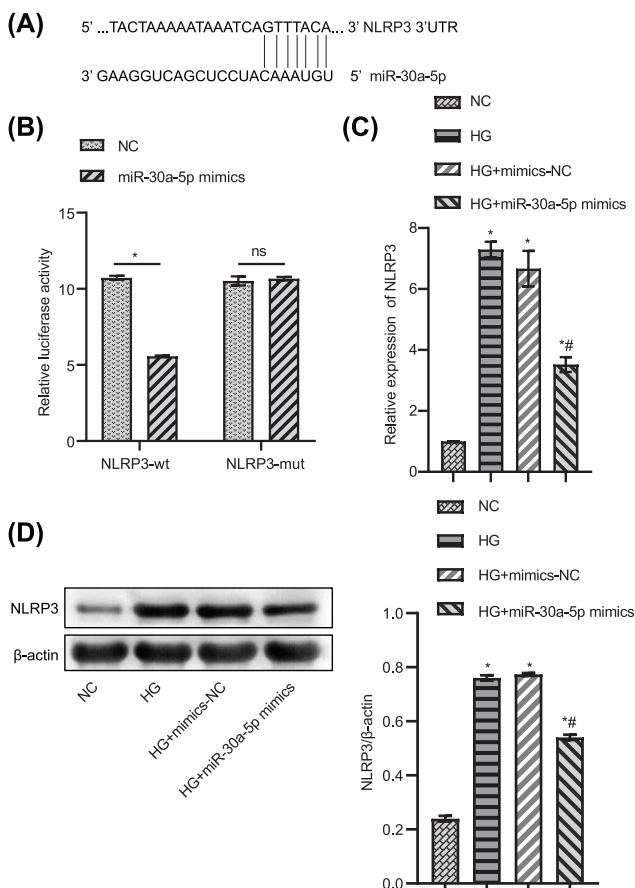


FIGURE 3. (continued)



**FIGURE 3.** Up-regulation of miR-30a-5p overexpression on high-glucose-induced podocyte injury. (A) miR-30a-5p level in each group was detected by RT-qPCR. (B) The cell viability of each group was measured by CCK-8. (C) Pyroptosis in each group was examined by flow cytometry. (D) The expression of caspase-1 and GSDMD-N was assayed by immunofluorescence in each group. Scale bar = 25  $\mu$ m. (E) Levels of TNF-alpha, IL-18, and IL-1beta in cell supernatant was surveyed by ELISA. \* vs. NC. # vs. HG.  $p < 0.05$ . Each assay was repeated three times, with three biological replicates. CCK-8, cell counting kit-8; RT-qPCR, Quantitative reverse transcription polymerase chain reaction; ELISA, enzyme-linked immunosorbent assay; GSDMD-N, gasdermin-N; IL-1 $\beta$ , interleukin-1beta; TNF, tumor necrosis factor.



**FIGURE 4.** NLRP3 directly targets miR-30a-5p. (A) Bioinformatic analysis predicted the target sequence of miR-30a-5p and NLRP3. (B) Luciferase assay was used to verify that NLRP3 directly targets miR-30a-5p. (C) RT-qPCR was used to explore the gene expression level of NLRP3. (D) Western blotting was used to determine NLRP3 protein level. \* vs. NC. # vs. HG.  $p < 0.05$ . Each assay was repeated three times, with three biological replicates. RT-qPCR, Quantitative reverse transcription polymerase chain reaction; NLRP3, NLR family pyrin domain containing 3.

in DN-mice and DN-podocyte. The percentage of pyroptosis also increased in DN-podocyte. Evidence show that inflammation participates in the occurrence and development of DN (Navarro-González *et al.*, 2011). For example, the inflammatory factor TNF- $\alpha$  induces apoptosis while directly damaging the kidney through cytotoxicity and is an important indicator of DN inflammation (Duran-Salgado & Rubio-Guerra, 2014). The accumulation of renal inflammatory cells was found in patients with DN and DN animal models, and the degree of inflammation was related to the progress of renal insufficiency (Chow *et al.*, 2004, Nguyen *et al.*, 2006). At the same time, in patients and animals with DN, the levels of pro-inflammatory cytokines in the renal tissue are also increased (Navarro *et al.*, 2006). This is consistent with our study findings. Collectively, pyroptosis and subsequent inflammation play an essential role in the occurrence and development of DN.

NLRP3 is the most studied inflammatory corpuscle and has been reported as a potential target for treating DN (Qiu & Tang, 2016). The activation of NLRP3 inflammatory corpuscles leads to the development of DN in diabetic mice (Shahzad *et al.*, 2015). Studies have also shown that inhibiting NLRP3 activation can improve DN injury (Zhang *et al.*, 2019, An *et al.*, 2020). NLRP3 indirectly regulates the maturation and secretion of IL-1beta and IL-18 by activating caspase-1, which leads to an inflammatory reaction. Activated caspase-1 can also cleave GSDMD to produce an N-terminal cleavage product (GSDMD-N), which can induce pyroptosis by forming pores in the plasma membrane (Shi *et al.*, 2015). This is consistent with our research results. Some studies have found that IL-22 has an excellent therapeutic effect on DN as it diminished the expression of NLRP3, caspase-1, and IL-1beta (Wang *et al.*, 2017). Our research found that overexpression of NLRP3 could increase pyroptosis-related proteins and pro-inflammatory cytokines in podocytes, increase the cell pyroptosis rate, and decrease cell viability in podocytes.

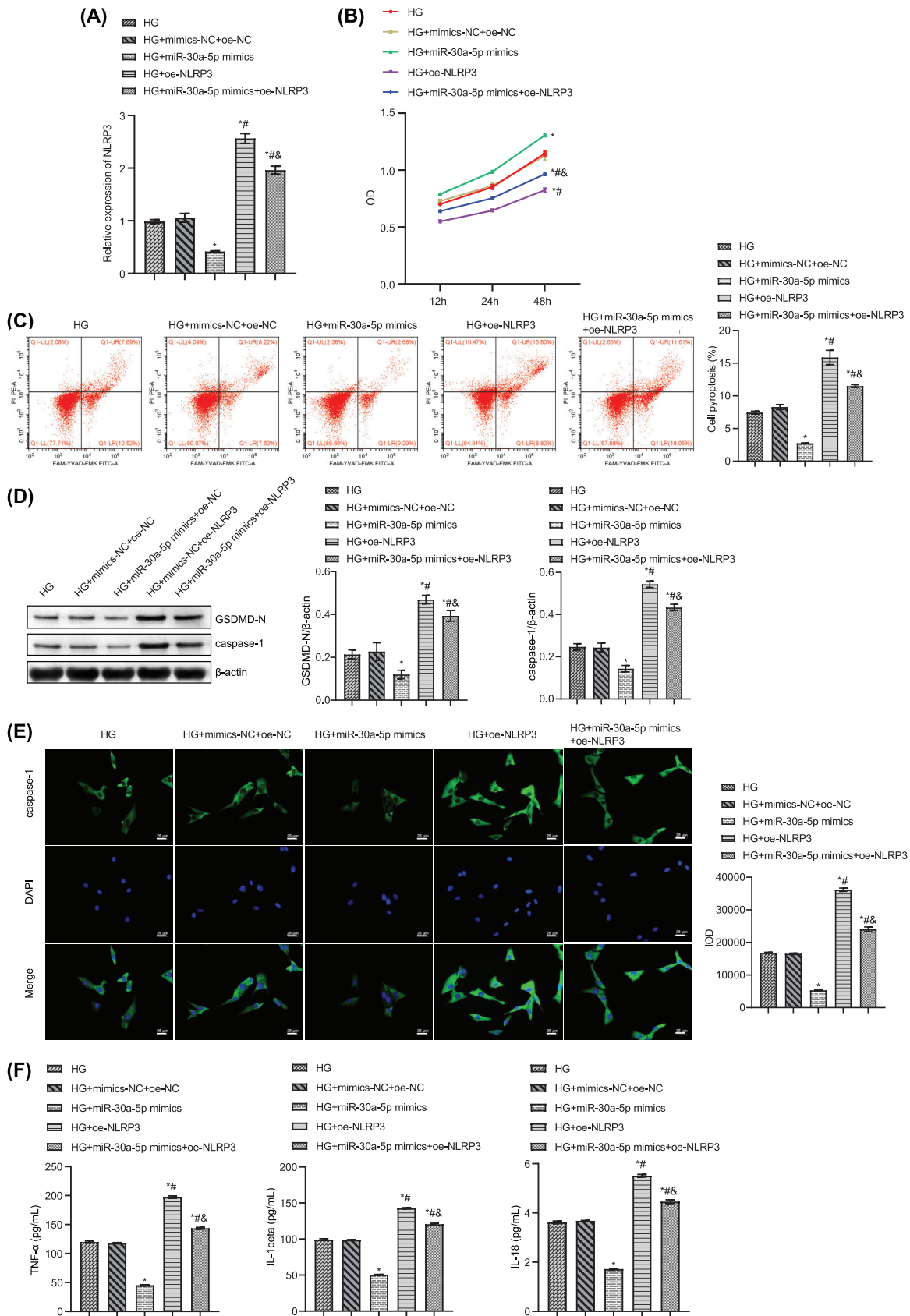


**FIGURE 5.** Overexpression of NLRP3 reverses the effects of miR-30a-5p at podocyte injury. (A) RT-qPCR detection for NLRP3 expression. (B) CCK8 assay was used to test cell viability. (C) Flow cytometry assay for podocyte pyroptosis. (D) Western blot for GSDMD-N and caspase-1 levels in podocytes. (E) The expression of caspase-1 was examined by immunofluorescence. Scale bar = 25  $\mu$ m. (F) The levels of TNF- $\alpha$ , IL-18, and IL-1 $\beta$  in the cell supernatant were measured by ELISA. \* vs. HG. # vs. HG+miR-30a-5p. & vs. HG+oe-NLRP3.  $p < 0.05$ . Each assay was repeated three times, with three biological replicates. CCK-8, cell counting kit-8; RT-qPCR, Quantitative reverse transcription polymerase chain reaction; ELISA, enzyme-linked immunosorbent assay; NLRP3, NLR family pyrin domain containing 3; GSDMD-N, gasdermin-N; IL-1 $\beta$ , interleukin-1beta; TNF, tumor necrosis factor.

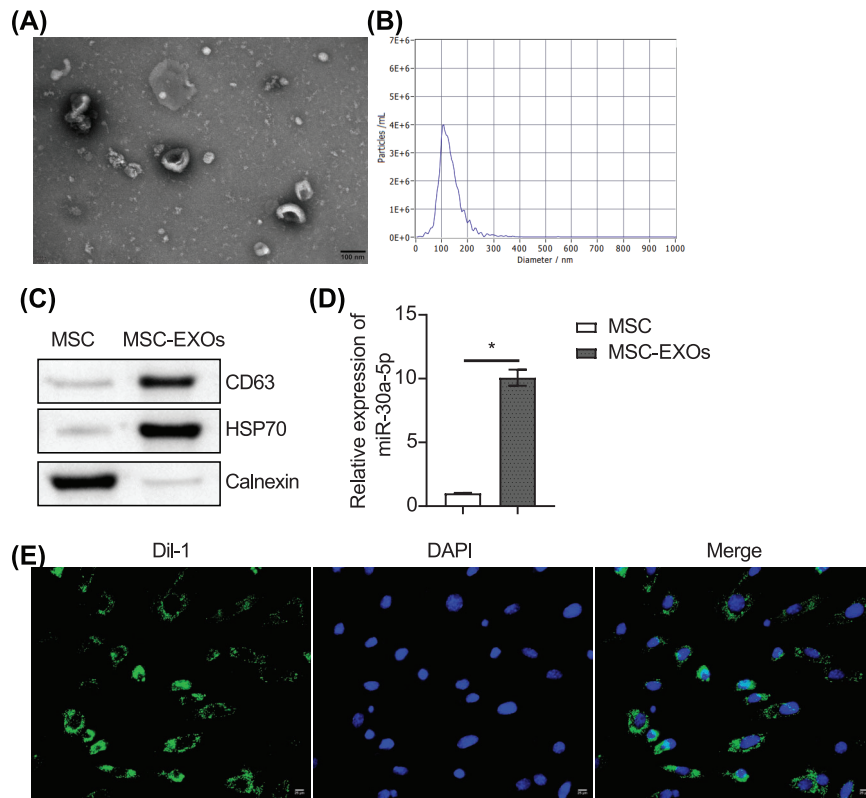


**FIGURE 6.** MSC-derived exosomal miR-30a-5p can be taken up by podocytes. (A and B) Exosomes were identified by TEM and NTA. © Analysis of CD63, HSP70 and calnexin expression in exosomes by western blot. (D) Expression of miR-30a-5p was detected by RT-qPCR © (E) Uptake assay of exosomes. Scale bar = 25  $\mu$ m. \* vs. MSC.  $p < 0.05$ . Each assay was repeated three times, with three biological replicates. RT-qPCR, Quantitative reverse transcription polymerase chain reaction; TEM, transmission electron microscopy; NTA, nanoparticle tracking analysis.

These findings suggest that the NLRP3/caspase-1/IL-1 $\beta$  axis plays an important role in DN.

Until now, conventional treatment strategies for DN have focused on renin-angiotensin-aldosterone system blockade, blood glucose level control, and weight loss (Doshi & Friedman, 2017; Cervantes et al., 2022). Commonly used first-in-line treatments are renin-angiotensin system inhibitors, including angiotensin-converting enzyme inhibitors and angiotensin receptor blockers (Tripathi & Yadav, 2013; Doshi & Friedman, 2017). Dapagliflozin, an inhibitor of sodium-glucose cotransporter-2, is often used as the first choice for DN treatment in clinical practice (Heerspink et al., 2020; Wheeler et al., 2021). However, these therapies have certain limitations and side effects. For instance, dapagliflozin treatment can lead to genital infections and increase the risk of bone fractures (Wang et al., 2019; Bansal et al., 2020). Therefore, there is an urgent need to explore and understand emerging and effective nephroprotective therapeutic strategies to slow the progression of DN. MSCs-derived exosomes have been shown to possess various therapeutic effects, such as tissue regeneration, wound healing, anti-tumor effects, and immune modulation (Joo et al., 2020). When tested in various disease models, MSC-derived exosomes display similar or even superior therapeutic abilities compared to their parent cells (Kastner et al., 2020; Maumus et al., 2020). MSC-derived exosomes also have the advantage of being

safe as they are considered non-immunogenic, with lower risks of host alloimmune rejection (Ankrum et al., 2014). Several studies have confirmed the potential of exosomes as therapeutic delivery vehicles for the treatment of DN (Peng et al., 2022). For example, exosomes loaded with miR-486-5p promote autophagy flux and inhibit apoptosis of podocytes through the Smad1/mTOR signaling pathway, thus attenuating DN (Jin et al., 2019). In another report, miR-25-3p, in an M2 macrophage-derived exosome, ameliorated HG-induced podocyte injury by activating autophagy and inhibiting the expression of dual specificity phosphatase 1 protein (Huang et al., 2020). Our study showed that exosomal miR-30a-5p inhibited HG-induced podocyte pyroptosis and inflammation by suppressing NLRP3 expression. This is the first study to investigate the effect of exosomal miR-30a-5p on podocyte pyroptosis in DN. The application of exosomes in therapy still faces some limitations. The content and accuracy of miRNA in exosomes are restricted by the preparation method and measurement tools (Chevillet et al., 2014). The level of miRNA in exosomes is regulated by upstream signaling pathways (Zhang et al., 2010). Exosomes therapy is limited by dosage, purity, and stability issues, and the yield, composition, and properties of extracellular vesicles depend on the cell growth conditions, cell type, and processing methods, which means that their quantity and therapeutic efficacy are restricted (Baek et al., 2019). Therefore, further

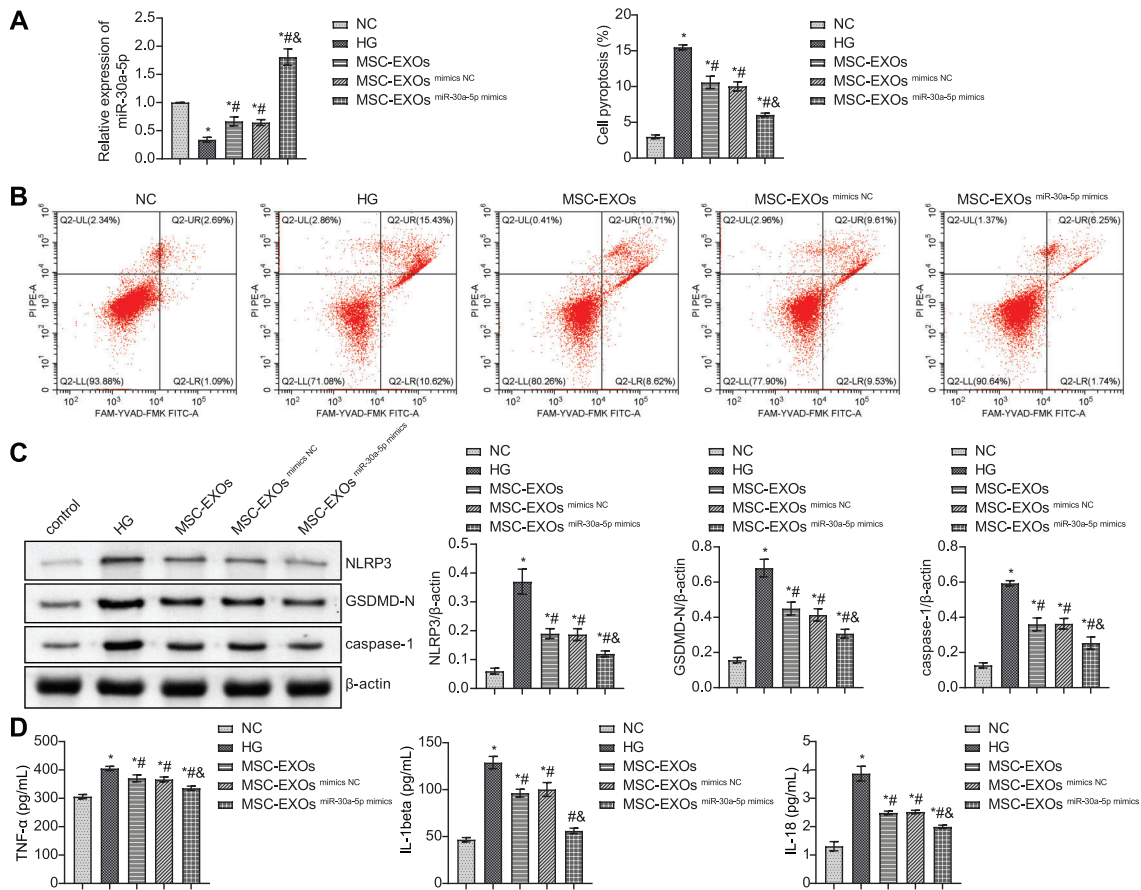


**FIGURE 7.** MSC-derived exosomes carrying miR-30a-5p inhibit podocyte pyroptosis by regulating NLRP3. (A) Transfection efficiency of miR-30a-5p mimics detected by RT-qPCR. (B) Flow cytometry detection for pyroptosis. (C) Western blot detection of NLRP3, GSDMD-N, and caspase-1 in podocytes. (D) ELISA to detect TNF- $\alpha$ , IL-18, and IL-1 $\beta$  expression in podocytes. \* vs. NC. # vs. HG. & vs. MSC-EXOs mimics NC.  $p < 0.05$ . Each assay was repeated three times, with three biological replicates. MSC, mesenchymal stem cell; RT-qPCR, Quantitative reverse transcription polymerase chain reaction; ELISA, enzyme-linked immunosorbent assay; NLRP3, NLR family pyrin domain containing 3; GSDMD-N, gsdmermin-N; IL-1 $\beta$ , interleukin-1beta; TNF, tumor necrosis factor.

research is needed to make exosome preparation more robust and effective and determine the optimal treatment strategy to overcome the limitations of exosome therapy.

Collectively, our study demonstrated that miR-30a-5p could diminish NLRP3 expression and mitigate podocyte pyroptosis. Meanwhile, MSCs-derived exosomes could be loaded with miR-30a-5p, thus regulating podocyte pyroptosis in DN. This would strengthen the validity of miR-30a-5p as a useful molecular target to reverse DN. Overall, these results provide evidence that pyroptosis-related pathways could be targeted for a novel therapeutic target of DN.

**Acknowledgement:** This work was supported by all the authors.

**Funding Statement:** The authors received no specific funding for this study.

**Author Contributions:** WL contributed to the concept and design of the study. WL and KG contributed to the acquisition of data. WL, DX, and ZX principally interpreted the data. WL wrote the original draft of the manuscript. All authors contributed toward revising the manuscript critically for important intellectual content, read and

approved the final version submitted for publication, and take responsibility for the statements made in the published article.

**Availability of Data and Materials:** The dates used to support the findings of this study are available from the corresponding author upon request.

**Ethical Approval:** All animal experiments complied with ARRIVE guidelines. This study was approved by the Hunan SJA Laboratory Animal Co., Ltd. (ethics approval number IACUC-SJA2021019-4).

**Conflicts of Interest:** The authors declare that the research was conducted in the absence of any commercial or financial relationships that could be construed as a potential conflict of interest.

## References

An X, Zhang Y, Cao Y, Chen J, Qin H, Yang L (2020). Punicalagin protects diabetic nephropathy by inhibiting pyroptosis based on TXNIP/NLRP3 pathway. *Nutrients* 12: 1516. <https://doi.org/10.3390/nu12051516>

- Ankrum JA, Ong JF, Karp JM (2014). Mesenchymal stem cells: Immune evasive, not immune privileged. *Nature Biotechnology* **32**: 252–260. <https://doi.org/10.1038/nbt.2816>
- Assady S, Wanner N, Skorecki KL, Huber TB (2017). New insights into podocyte biology in glomerular health and disease. *Journal of the American Society of Nephrology* **28**: 1707–1715. <https://doi.org/10.1681/ASN.2017010027>
- Baek G, Choi H, Kim Y, Lee HC, Choi C (2019). Mesenchymal stem cell-derived extracellular vesicles as therapeutics and as a drug delivery platform. *Stem Cells Translational Medicine* **8**: 880–886. <https://doi.org/10.1002/sctm.18-0226>
- Bansal G, Thanikachalam PV, Maurya RK, Chawla P, Ramamurthy S (2020). An overview on medicinal perspective of thiazolidine-2,4-dione: A remarkable scaffold in the treatment of type 2 diabetes. *Journal of Advanced Research* **23**: 163–205. <https://doi.org/10.1016/j.jare.2020.01.008>
- Bartel DP (2004). MicroRNAs: Genomics, biogenesis, mechanism, and function. *Cell* **116**: 281–297. [https://doi.org/10.1016/S0092-8674\(04\)00045-5](https://doi.org/10.1016/S0092-8674(04)00045-5)
- Caserta S, Mengozzi M, Kern F, Newbury SF, Ghezzi P, Llewelyn MJ (2017). Severity of systemic inflammatory response syndrome affects the blood levels of circulating inflammatory-relevant MicroRNAs. *Frontiers in Immunology* **8**: 1977. <https://doi.org/10.3389/fimmu.2017.01977>
- Cervantes CE, Hanouneh M, Jaar BG (2022). From screening to treatment: The new landscape of diabetic kidney disease. *BMC Medicine* **20**: 329. <https://doi.org/10.1186/s12916-022-02537-4>
- Chevillet JR, Kang Q, Ruf IK, Briggs HA, Vojtech LN et al. (2014). Quantitative and stoichiometric analysis of the microRNA content of exosomes. *Proceedings of the National Academy of Sciences of the United States of America* **111**: 14888–14893. <https://doi.org/10.1073/pnas.1408301111>
- Chow FY, Nikolic-Paterson DJ, Atkins RC, Tesch GH (2004). Macrophages in streptozotocin-induced diabetic nephropathy: Potential role in renal fibrosis. *Nephrology, Dialysis, Transplantation* **19**: 2987–2996. <https://doi.org/10.1093/ndt/gfh441>
- Cui C, Zang N, Song J, Guo X, He Q et al. (2022). Exosomes derived from mesenchymal stem cells attenuate diabetic kidney disease by inhibiting cell apoptosis and epithelial-to-mesenchymal transition via miR-424-5p. *FASEB Journal* **36**: e22517. <https://doi.org/10.1096/fj.202200488R>
- Dieter C, Assmann TS, Costa AR, Canani LH, de Souza BM, Bauer AC, Crispim D (2019). MiR-30e-5p and MiR-15a-5p expressions in plasma and urine of type 1 diabetic patients with diabetic kidney disease. *Frontiers in Genetics* **10**: 563. <https://doi.org/10.3389/fgene.2019.00563>
- Ding X, Jing N, Shen A, Guo F, Song Y et al. (2020). MiR-21-5p in macrophage-derived extracellular vesicles affects podocyte pyroptosis in diabetic nephropathy by regulating A20. *Journal of Endocrinological Investigation* **44**: 1175–1184. <https://doi.org/10.1007/s40618-020-01401-7>
- Doshi SM, Friedman AN (2017). Diagnosis and management of type 2 diabetic kidney disease. *Clinical Journal of the American Society of Nephrology* **12**: 1366–1373. <https://doi.org/10.2215/CJN.11111016>
- Duran-Salgado MB, Rubio-Guerra AF (2014). Diabetic nephropathy and inflammation. *World Journal of Diabetes* **5**: 393–398. <https://doi.org/10.4239/wjd.v5.i3.393>
- Eulalio A, Huntzinger E, Izaurralde E (2008). Getting to the root of miRNA-mediated gene silencing. *Cell* **132**: 9–14. <https://doi.org/10.1016/j.cell.2007.12.024>
- Filipowicz W, Bhattacharyya SN, Sonenberg N (2008). Mechanisms of post-transcriptional regulation by microRNAs: Are the answers in sight? *Nature Reviews. Genetics* **9**: 102–114. <https://doi.org/10.1038/nrg2290>
- Gao Y, Ma Y, Xie D, Jiang H (2022). ManNAc protects against podocyte pyroptosis via inhibiting mitochondrial damage and ROS/NLRP3 signaling pathway in diabetic kidney injury model. *International Immunopharmacology* **107**: 108711. <https://doi.org/10.1016/j.intimp.2022.108711>
- Hao Y, Miao J, Liu W, Cai K, Huang X, Peng L (2021). Mesenchymal stem cell-derived exosomes carry MicroRNA-125a to protect against diabetic nephropathy by targeting histone deacetylase 1 and downregulating endothelin-1. *Diabetes, Metabolic Syndrome and Obesity* **14**: 1405–1418. <https://doi.org/10.2147/DMSO.S286191>
- He X, Kuang G, Wu Y, Ou C (2021). Emerging roles of exosomal miRNAs in diabetes mellitus. *Clinical and Translational Medicine* **11**: e468. <https://doi.org/10.1002/ctm2.468>
- Heerspink HJL, Stefánsson BV, Correa-Rotter R, Chertow GM, Greene T et al. (2020). Dapagliflozin in patients with chronic kidney disease. *The New England Journal of Medicine* **383**: 1436–1446. <https://doi.org/10.1056/NEJMoa2024816>
- Hong Q, Zhang L, Das B, Li Z, Liu B et al. (2018). Increased podocyte Sirtuin-1 function attenuates diabetic kidney injury. *Kidney International* **93**: 1330–1343. <https://doi.org/10.1016/j.kint.2017.12.008>
- Huang H, Liu H, Tang J, Xu W, Gan H, Fan Q, Zhang W (2020). M2 macrophage-derived exosomal miR-25-3p improves high glucose-induced podocytes injury through activation autophagy via inhibiting DUSP1 expression. *IUBMB Life* **72**: 2651–2662. <https://doi.org/10.1002/iub.2393>
- Ito Y, Hsu MF, Bettaieb A, Koike S, Mello A, Calvo-Rubio M, Villalba JM, Haj FG (2017). Protein tyrosine phosphatase 1B deficiency in podocytes mitigates hyperglycemia-induced renal injury. *Metabolism-Clinical and Experimental* **76**: 56–69. <https://doi.org/10.1016/j.metabol.2017.07.009>
- Jiang Z, Hou Z, Li L, Liu W, Yu Z, Chen S (2021). Exosomal circEPB41L2 serves as a sponge for miR-21-5p and miR-942-5p to suppress colorectal cancer progression by regulating the PTEN/AKT signalling pathway. *European Journal of Clinical Investigation* **51**: e13581. <https://doi.org/10.1111/eci.13581>
- Jin J, Shi Y, Gong J, Zhao L, Li Y, He Q, Huang H (2019). Exosome secreted from adipose-derived stem cells attenuates diabetic nephropathy by promoting autophagy flux and inhibiting apoptosis in podocyte. *Stem Cell Research and Therapy* **10**: 95. <https://doi.org/10.1186/s13287-019-1177-1>
- Joo HS, Suh JH, Lee HJ, Bang ES, Lee JM (2020). Current knowledge and future perspectives on mesenchymal stem cell-derived exosomes as a new therapeutic agent. *International Journal of Molecular Sciences* **21**: 727. <https://doi.org/10.3390/ijms21030727>
- Kastner N, Mester-Tonczar J, Winkler J, Traxler D, Spannbaauer A, Ruger BM, Goliash G, Pavo N, Gyongyosi M, Zlabinger K (2020). Comparative effect of MSC Secretome to MSC Co-culture on cardiomyocyte gene expression under hypoxic conditions *in vitro*. *Frontiers in Bioengineering and Biotechnology* **8**: 502213. <https://doi.org/10.3389/fbioe.2020.502213>

- Lal MA, Patrakka J (2018). Understanding podocyte biology to develop novel kidney therapeutics. *Frontiers in Endocrinology* **9**: 409. <https://doi.org/10.3389/fendo.2018.00409>
- Lang Y, Zhao Y, Zheng C, Lu Y, Wu J et al. (2019). MiR-30 family prevents uPAR-ITGB3 signaling activation through calcineurin-NFATC pathway to protect podocytes. *Cell Death and Disease* **10**: 401. <https://doi.org/10.1038/s41419-019-1625-y>
- Liu WT, Peng FF, Li HY, Chen XW, Gong WQ et al. (2016). Metadherin facilitates podocyte apoptosis in diabetic nephropathy. *Cell Death Discovery* **7**: e2477–e2477. <https://doi.org/10.1038/cddis.2016.335>
- Liu P, Zhang Z, Li Y (2021). Relevance of the pyroptosis-related inflammasome pathway in the pathogenesis of diabetic kidney disease. *Frontiers in Immunology* **12**: 603416. <https://doi.org/10.3389/fimmu.2021.603416>
- Mamun AA, Wu Y, Nasrin F, Akter A, Taniya MA, Munir F, Jia C, Xiao J (2021). Role of pyroptosis in diabetes and its therapeutic implications. *Journal of Inflammation Research* **14**: 2187–2206. <https://doi.org/10.2147/JIR.S291453>
- Man SM, Karki R, Kanneganti TD (2017). Molecular mechanisms and functions of pyroptosis, inflammatory caspases and inflammasomes in infectious diseases. *Immunological Reviews* **277**: 61–75. <https://doi.org/10.1111/imr.12534>
- Maumus M, Rozier P, Boulestreau J, Jorgensen C, Noël D (2020). Mesenchymal stem cell-derived extracellular vesicles: Opportunities and challenges for clinical translation. *Frontiers in Bioengineering and Biotechnology* **8**: 997. <https://doi.org/10.3389/fbioe.2020.00997>
- Miranda K, Yang X, Bam M, Murphy EA, Nagarkatti PS, Nagarkatti M (2018). MicroRNA-30 modulates metabolic inflammation by regulating Notch signaling in adipose tissue macrophages. *International Journal of Obesity* **42**: 1140–1150. <https://doi.org/10.1038/s41366-018-0114-1>
- Najafian B, Alpers CE, Fogo AB (2011). Pathology of human diabetic nephropathy. *Contributions to Nephrology* **170**: 36–47. <https://doi.org/10.1159/issn.0302-5144>
- Navarro JF, Milena FJ, Mora C, León C, García J (2006). Renal pro-inflammatory cytokine gene expression in diabetic nephropathy: Effect of angiotensin-converting enzyme inhibition and pentoxifylline administration. *American Journal of Nephrology* **26**: 562–570. <https://doi.org/10.1159/000098004>
- Navarro-González JF, Mora-Fernández C, Muros de Fuentes M, García-Pérez J (2011). Inflammatory molecules and pathways in the pathogenesis of diabetic nephropathy. *Nature Reviews. Nephrology* **7**: 327–340. <https://doi.org/10.1038/nrneph.2011.51>
- Nguyen D, Ping F, Mu W, Hill P, Atkins RC, Chadban SJ (2006). Macrophage accumulation in human progressive diabetic nephropathy. *Nephrology* **11**: 226–231. <https://doi.org/10.1111/j.1440-1797.2006.00576.x>
- Pavenstädt H, Kriz W, Kretzler M (2003). Cell biology of the glomerular podocyte. *Physiological Reviews* **83**: 253–307. <https://doi.org/10.1152/physrev.00020.2002>
- Peng L, Chen Y, Shi S, Wen H (2022). Stem cell-derived and circulating exosomal microRNAs as new potential tools for diabetic nephropathy management. *Stem Cell Research and Therapy* **13**: 25. <https://doi.org/10.1186/s13287-021-02696-w>
- Podgórski P, Konieczny A, Lis Ł., Witkiewicz W, Hruby Z (2019). Glomerular podocytes in diabetic renal disease. *Advances in Clinical and Experimental Medicine* **28**: 1711–1715. <https://doi.org/10.17219/acem/104534>
- Qiu YY, Tang LQ (2016). Roles of the NLRP3 inflammasome in the pathogenesis of diabetic nephropathy. *Pharmacological Research* **114**: 251–264. <https://doi.org/10.1016/j.phrs.2016.11.004>
- Raval N, Kumawat A, Kalyane D, Kalia K, Tekade RK (2020). Understanding molecular upsets in diabetic nephropathy to identify novel targets and treatment opportunities. *Drug Discovery Today* **25**: 862–878. <https://doi.org/10.1016/j.drudis.2020.01.008>
- Shahzad K, Bock F, Al-Dabet MM, Gadi I, Kohli S et al. (2016). Caspase-1, but not caspase-3, promotes diabetic nephropathy. *Journal of the American Society of Nephrology* **27**: 2270–2275. <https://doi.org/10.1681/ASN.2015060676>
- Shahzad K, Bock F, Dong W, Wang H, Kopf S et al. (2015). Nlrp3-inflammasome activation in non-myeloid-derived cells aggravates diabetic nephropathy. *Kidney International* **87**: 74–84. <https://doi.org/10.1038/ki.2014.271>
- Shi J, Zhao Y, Wang K, Shi X, Wang Y et al. (2015). Cleavage of GSDMD by inflammatory caspases determines pyroptotic cell death. *Nature* **526**: 660–665. <https://doi.org/10.1038/nature15514>
- Tesch GH (2017). Diabetic nephropathy—Is this an immune disorder? *Clinical Science* **131**: 2183–2199. <https://doi.org/10.1042/CS20160636>
- Tripathi YB, Yadav D (2013). Diabetic nephropathy: Causes and managements. *Recent Patents on Endocrine, Metabolic & Immune Drug Discovery* **7**: 57–64. <https://doi.org/10.2174/187221413804660971>
- Umanath K, Lewis JB (2018). Update on diabetic nephropathy: Core curriculum 2018. *American Journal of Kidney Diseases* **71**: 884–895. <https://doi.org/10.1053/j.ajkd.2017.10.026>
- Wang JY, Cheng YZ, Yang SL, An M, Zhang H, Chen H, Yang L (2019). Dapagliflozin attenuates hyperglycemia related osteoporosis in ZDF rats by alleviating hypercalciuria. *Frontiers in Endocrinology* **10**: 700. <https://doi.org/10.3389/fendo.2019.00700>
- Wang S, Li Y, Fan J, Zhang X, Luan J et al. (2017). Interleukin-22 ameliorated renal injury and fibrosis in diabetic nephropathy through inhibition of NLRP3 inflammasome activation. *Cell Death and Disease* **8**: e2937–e2937. <https://doi.org/10.1038/cddis.2017.292>
- Wang H, Lv D, Jiang S, Hou Q, Zhang L et al. (2022). Complement induces podocyte pyroptosis in membranous nephropathy by mediating mitochondrial dysfunction. *Cell Death and Disease* **13**: 281. <https://doi.org/10.1038/s41419-022-04737-5>
- Wharram BL, Goyal M, Wiggins JE, Sanden SK, Hussain S et al. (2005). Podocyte depletion causes glomerulosclerosis: Diphtheria toxin-induced podocyte depletion in rats expressing human diphtheria toxin receptor transgene. *Journal of the American Society of Nephrology* **16**: 2941–2952. <https://doi.org/10.1681/ASN.2005010055>
- Wheeler DC, Stefánsson BV, Jongs N, Chertow GM, Greene T et al. (2021). Effects of dapagliflozin on major adverse kidney and cardiovascular events in patients with diabetic and non-diabetic chronic kidney disease: A prespecified analysis from the DAPA-CKD trial. *Lancet Diabetes and Endocrinology* **9**: 22–31. [https://doi.org/10.1016/S2213-8587\(20\)30369-7](https://doi.org/10.1016/S2213-8587(20)30369-7)
- Wu J, Zheng C, Fan Y, Zeng C, Chen Z et al. (2014). Downregulation of microRNA-30 facilitates podocyte injury and is prevented

- by glucocorticoids. *Journal of the American Society of Nephrology* **25**: 92–104. <https://doi.org/10.1681/ASN.2012111101>
- Xin R, Sun X, Wang Z, Yuan W, Jiang W et al. (2018). Apocynin inhibited NLRP3/XIAP signalling to alleviate renal fibrotic injury in rat diabetic nephropathy. *Biomedicine & Pharmacotherapy* **106**: 1325–1331. <https://doi.org/10.1016/j.biopha.2018.07.036>
- Xiong J, Hu H, Guo R, Wang H, Jiang H (2021). Mesenchymal stem cell exosomes as a new strategy for the treatment of diabetes complications. *Frontiers in Endocrinology* **12**: 646233. <https://doi.org/10.3389/fendo.2021.646233>
- Yang Y, Fu L, Chen C, Hu M (2022). miRNA-148b-3p targeting SOCS3 inhibits macrophage M2 polarization by JAK2/STAT3 pathway in immune thrombocytopenia. *BIOCELL* **46**: 1319–1328. <https://doi.org/10.32604/biocell.2022.015760>
- Yang X, Yang M, Chen Y, Qian Y, Fei X, Gong C, Wang M, Xie X, Wang Z (2021). miR-30a-5p targets Becn1 to ameliorate high-glucose-induced glomerular podocyte injury in immortalized rat podocyte cell line. *American Journal of Translational Research* **13**: 1516–1525.
- Yarahmadi A, Shahrokhi SZ, Mostafavi-Pour Z, Azarpira N (2021). MicroRNAs in diabetic nephropathy: From molecular mechanisms to new therapeutic targets of treatment. *Biochemical Pharmacology* **189**: 114301. <https://doi.org/10.1016/j.bcp.2020.114301>
- Yu ZW, Zhang J, Li X, Wang Y, Fu YH, Gao XY (2020). A new research hot spot: The role of NLRP3 inflammasome activation, a key step in pyroptosis, in diabetes and diabetic complications. *Life Sciences* **240**: 117138. <https://doi.org/10.1016/j.lfs.2019.117138>
- Zhang Y, Cai Y, Zhang H, Zhang J, Zeng Y et al. (2021). Brown adipose tissue transplantation ameliorates diabetic nephropathy through the miR-30b pathway by targeting Runx1. *Metabolism-Clinical and Experimental* **125**: 154916. <https://doi.org/10.1016/j.metabol.2021.154916>
- Zhang Y, Liu D, Chen X, Li J, Li L et al. (2010). Secreted monocytic miR-150 enhances targeted endothelial cell migration. *Molecular Cell* **39**: 133–144. <https://doi.org/10.1016/j.molcel.2010.06.010>
- Zhang R, Qin Land, Shi J (2020). MicroRNA-199a-3p suppresses high glucose-induced apoptosis and inflammation by regulating the IKK $\beta$ /NF- $\kappa$ B signaling pathway in renal tubular epithelial cells. *International Journal of Molecular Medicine* **46**: 2161–2171. <https://doi.org/10.3892/ijmm.2020.4751>
- Zhang C, Zhu X, Li L, Ma T, Shi M, Yang Yand, Fan Q (2019). A small molecule inhibitor MCC950 ameliorates kidney injury in diabetic nephropathy by inhibiting NLRP3 inflammasome activation. *Diabetes, Metabolic Syndrome and Obesity* **12**: 1297–1309. <https://doi.org/10.2147/DMSO>
- Zhao Y, Wu J, Zhang M, Zhou M, Xu F et al. (2017a). Angiotensin II induces calcium/calcineurin signaling and podocyte injury by downregulating microRNA-30 family members. *Journal of Molecular Medicine* **95**: 887–898. <https://doi.org/10.1007/s00109-017-1547-z>
- Zhao Y, Yin Z, Li H, Fan J, Yang S, Chen C, Wang DW (2017b). MiR-30c protects diabetic nephropathy by suppressing epithelial-to-mesenchymal transition in db/db mice. *Aging Cell* **16**: 387–400. <https://doi.org/10.1111/accel.12563>
- Zuo Y, Chen L, Gu H, He X, Ye Z, Wang Z, Shao Q, Xue C (2021). GSDMD-mediated pyroptosis: A critical mechanism of diabetic nephropathy. *Expert Reviews in Molecular medicine* **23**: e23. <https://doi.org/10.1017/erm.2021.27>